Higher-mode Textile Patch Antenna with Embroidered Vias for On-body Communication

A. Paraskevopoulos[1,2*], D.S. Fonseca[1], R.D. Seager[1], W.G. Whittow[1], J.C. Vardaxoglou[1], A.A. Alexandridis[2]

[1]School of Electronic, Electrical and Systems Engineering, Loughborough University, Loughborough, UK
[2]Institute of Informatics & Telecommunications,, National Centre for Scientific Research "Demokritos", Athens, Greece
[*]A.Paraskevopoulos@lboro.ac.uk

Abstract: This paper presents a wearable textile higher-mode microstrip patch antenna (HMMPA) that has been designed to radiate omni-directionally at 2.4 GHz ISM band. Emphasis is given to the fabrication process of the textile vias with conductive sewing thread that play an important role in generating the optimal mode for on-body radiation. The embroidery technique enabled a side-fed low-profile antenna which could be placed directly against the body. The proposed textile HMMPA antenna performance is compared with a probe-fed HMMPA antenna fabricated with rigid copper radiating parts, for both free space and on-body conditions. The on-body antenna performance has been tested by performing near-field measurements of the antenna on a full-body specific anthropomorphic mannequin (SAM) phantom in an anechoic chamber. Results show that the proposed textile HMMPA antenna with vias made from conductive thread can radiate on-body with good efficiency while minimising the radiation in the broadside direction.

1. Introduction

In the last decade, there is a growing interest in the development of wearable devices for on-body and off-body wireless communications systems. Some remarkable low-profile, flexible and conformal to the body textile antenna designs have been proposed in the literature [1–9]. According to Hall [10], it has been proven that antennas with normal to human body polarisation generate a strong surface wave propagation mode that is practical for on-body communication. As such, a higher-mode microstrip patch antenna (HMMPA) was initially proposed by Delaveaud in [11] and was later adopted to on-body communications by Scanlon [12].

In a number of cases, shorting vias have been used for the excitation of the monopole-like propagation mode in the form of copper vias in rigid patch antennas [11–18] or embroidered vias in fabric patch antenna realisations [5, 7–9, 19, 20]. In [19], different shorting techniques have been tested through EM simulations. It was shown that by using embroidered conductive yarn instead of silver fabric and PEC, radiation gain dropped about 2.6 dB at 4.5 GHz while radiation efficiency reduced 2.8 dB. This attributed to high conductor losses, although the performance was improved for higher frequencies.

In a recent study, a textile circular patch antenna has been proposed with a thickness profile of 1 mm and textile embroidered shorting vias [20]. For the feeding via, a coaxial connector was used instead of a conductive thread via that introduces a non-textile part in the design. In the same study, a rectangular muscle equivalent phantom was used, which is a simplified approximation of a real human body, without considering scattering and shadowing effects from different body parts. The probe-fed design of the proposed antenna makes it impractical to be measured directly on a real human body and the achieved relatively low on-body efficiency(14%) leaves room for further design improvement.

In this paper, a fully-textile higher-mode microstrip patch antenna (HMMPA) is proposed and compared with a previously developed HMMPA [21], [22] with copper sheet and metallic pins. The excitation of the desired mode is obtained by utilising embroidered vias with conductive thread for the central feeding and for the shorting parts up to the ground plane. This is the first time that a fully flexible textile HMMPA antenna for on-body communications is implemented without any rigid parts. The main challenge was to ensure that a perfect connection between the patch and the ground plane can be formed with embroidered vias and test how the low conductivity of the vias can affect the antenna efficiency.

This paper is organised as follows: in Section II the proposed multilayer HMMPA antenna design is presented together with some fabrication challenges. A perpendicular to body polarisation and surface wave propagation are shown through EM simulation. In Section III the measurement results are discussed in detail regarding the impedance matching, radiation characteristics and far-field patterns. At last, in Section IV conclusions are drawn.

2. Antenna Design and Fabrication Process

2.1. Antenna Design

The benefits of the textile HMMPA antenna over the copper HMMPA antenna are twofold. At first, the new design is made all-textile without any rigid copper parts adding more flexibility and enabling the automation of the fabrication process using the embroidery machine. Secondly, the multilayer design provides side feeding capability keeping the total thickness at 0.4 cm while the previous probe-fed design of the copper HMMPA antenna results in a total thickness of 1.4 cm. The multilayer side-fed design enables to be closely attached and measured directly on the human body.

In Fig. 1 the proposed textile HMMPA antenna together with the copper HMMPA antenna are displayed. The optimised antenna dimensions as simulated in CST Microwave Studio are shown in Fig. 2a, as resulted from the EM simulations. The multilayer antenna exploded 3D view is shown in Fig. 2b. It is comprised of four layers: the top patch, the dielectric felt material, the transmission line on top of a thin felt material and the ground plane.

The theoretical electric field amplitude distribution (TM_{21} mode) below the radiating patch is drawn in Fig. 3. It is observed that in X-axis direction, the electric field varies by one full cycle while in the Y-axis varies by half cycle due to the nodes and peaks forced by the shorting vias and the feeding via respectively.

The proposed patch antenna is selected instead of other antenna types as the optimal choice for maximising on-body propagation. It can be comfortably worn and embedded in clothing due to its unobtrusive low-profile design.

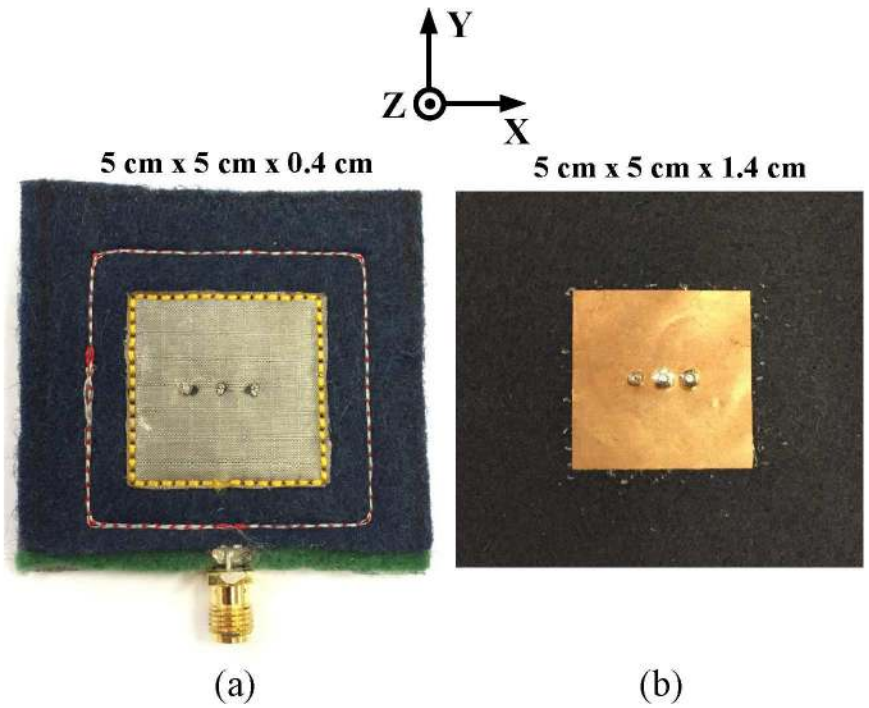

Fig. 1. *(a) Fully-textile HMMPA antenna fabricated on the embroidery machine, (b) HMMPA antenna using copper sheet and metallic vias*

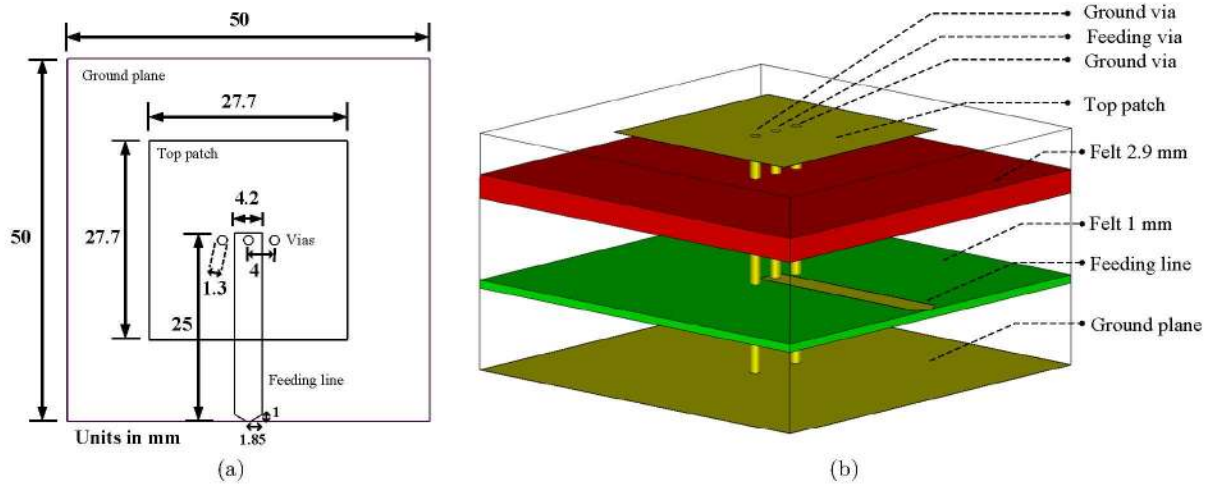

Fig. 2. *Textile HMMPA antenna design: (a) Dimensions and (b) exploded 3D view*

The TM_{21} mode enables the patch antenna to radiate omni-directionally with polarisation normal to the body surface. This polarisation can be also achieved from a wire monopole antenna, placed normal to the body surface, however due to its height is impractical for wearable applications. The desired mode is excited by using two shorting vias at an offset distance from the centre feed. A miniaturisation of the patch radiator to less than $\lambda/4$ instead of $\lambda/2$ at the fundamental (TM_{01}) mode is achieved. This leads to an overall size of 5 cm x 5 cm x 0.4 cm at the 2.4 GHz ISM band.

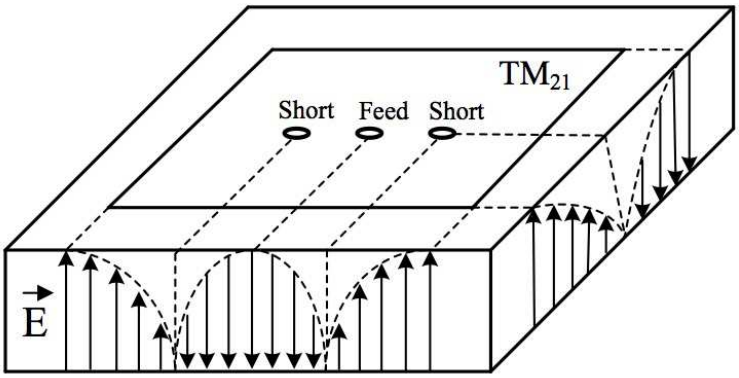

Fig. 3. *Theoretical electric field distribution of the TM_{21} mode of HMMPA antenna*

Other textile antenna types, such as PIFA or planar monopole antennas that achieve an omnidirectional radiation pattern are found in the literature [2, 23]. The textile PIFA, exhibits a comparable on-body efficiency with the HMMPA up to 40%, although it fails to generate a strong surface wave propagation. As far as a textile monopole is concerned, due to the lack of a large ground plane, the radiation pattern is distorted when placed on the body surface.

The proposed antenna can excite a strong surface or creeping wave propagation mode that results in good coverage around the body surface, reducing the path loss and minimising fading in on-body channels. Some possible applications, that are favoured from the strong on-body wave propagation of the textile HMMPA antenna, can be found in:

- *Medical and fitness applications*: where many vital signs sensor readings need to be collected from a central unit hub placed on the user's body surface.
- *Military and space applications*: where several wearable devices need to communicate with an off-body access point via an on-body central relay device.
- *Personal entertainment*, where, for example, wireless headphones or a smart watch need to be connected with a mobile terminal placed on the surface of the human body.

2.2. EM Simulation of Antenna on the Human Body

In this section, the suitability of the designed textile HMMPA antenna for on-body communications is examined. An EM simulation of the textile HMMPA antenna on the body was employed. The numerical model had the same geometrical and dielectric characteristics as the actual SAM phantom with homogeneous dielectric material emulating an average of human body tissues of $\epsilon_r = 35.4$ and $\sigma = 1.81$ S/m at 2.412 GHz.

In Fig. 4a, the normalised electric field vector in a cross section through the centre of the chest is illustrated. A perpendicular to body electric field polarisation is achieved which is essential for the generation of surface wave propagation [10]. In addition, the magnitude of the electric field distribution of the proposed antenna around and along the body surface is shown in Fig. 4b and Fig. 4c respectively. The diffraction of the propagated electric field on the body curvature is apparent. A monopole-like propagation is obtained which enables the on-body communication between low-profile wearable antennas.

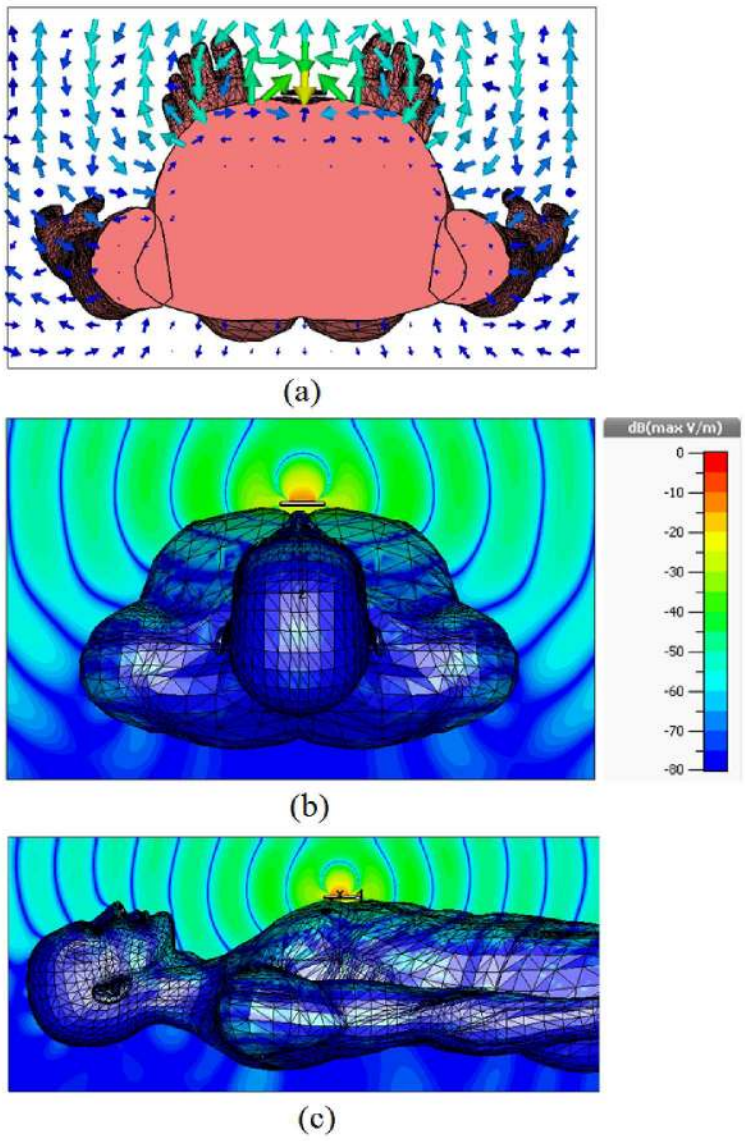

Fig. 4. *(a) Normalised electric field vector of HMMPA antenna in a cross section of SAM phantom derived from EM simulation. Normalised electric field amplitude (b) around and (c) along SAM phantom*

2.3. Fabric Materials

For the creation of the antenna two conductive materials were used, Nora-Dell [25] and Liberator-20 [26]. Nora-Dell is a conductive metallized nylon fabric coated with nickel and silver that form a highly conducting flexible sheet created by Shieldex. It exhibits the same durability as fully embroidered designs, while having higher conductivity. An average surface resistivity of 0.005 $\Omega/square$ according to the datasheet [25] is given (an approximate conductivity of 1.54×10^6 S/m for 0.13 mm of Nora-Dell thickness). It was used to create the top patch, the transmission line and the ground plane conductive parts. Liberator 20 is a 20 filament conductive thread created by Syscom Advanced Materials, Inc. Each filament has a diameter of 0.22 mm with a Vectran fiber core and is metallised with silver coating,

with a DC linear resistance of around 2 Ω/ft, or an approximate conductivity of 4.5×10^7 S/m. This was used to embroider the vias that connect the top patch to the microstrip line and the ground plane.

Felt material was used as a dielectric for both the transmission line and the antenna, with permittivity and loss tangent measured in a split-post dielectric resonator. For the 1mm felt, $\epsilon_r = 1.2$ and $\tan\delta = 0.0013$ was measured while for the 2.9mm felt dielectric $\epsilon_r = 1.185$ and $\tan\delta = 0.0012$.

2.4. Embroidery Process

There are three major components that need to be embroidered, the central via from the top patch to the feeding microstrip and the side vias from the top patch to the bottom ground plane.

It is important to keep the exact distance between the shorting vias and the centre feeding via, at 4 mm. This distance would directly influence the antenna impedance matching as well as the proper excitation of the desired TM_{21} mode and consequently its radiation pattern. Via diameter could influence the antenna performance as well. This should be 1.3 mm as resulted from the EM simulation and the previously fabricated copper HMMPA antenna. To achieve this, the embroidered vias were stitched by using several threads.

Shown in Figure 5 are the via models which were tested in order to obtain the exact diameter and distance between the embroidered vias. For the first three models, the sewing method was set to Satin Stitch, with the density starting at 2lines/mm to 3lines/mm and finally 4.5lines/mm. For the last three models, the sewing method was set to Concentric Circle Stitch and the density was set to 2, 2.5 and 3 lines/mm. After testing and measuring the resulting density, we concluded to embroider the HMMPA antenna using the 6th via model.

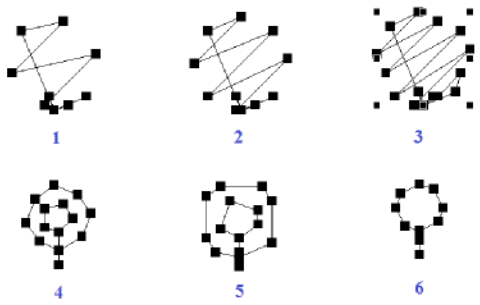

Fig. 5. *Via models with different sewing methods and stitch density*

The stages of the embroidery process are described here in detail. The first step was to stitch the central via through the Nora-Dell patch, the dielectric to the microstrip line with Liberator, this will create the feed via and hold the patch and microstrip in place for the rest of the process. Since the via goes through the bottom side of felt it could make contact with the ground plane. To prevent this, a small bit of masking tape was used to cover the bottom of the via preventing contact with the ground plane.

The next step was to attach the Nora-Dell to the bottom of the design and stitch the side vias using Liberator. Since the embroidery machine is not made to handle conductive thread, there was a high risk that the Liberator thread could unravel and break during the

stitching process. To reduce this effect, a small portion of oil was applied to the thread while it was being stitched. This made the individual thread filaments stick together and unravel less. After this, the whole design was secured in place by embroidering the perimeter of the patch and ground plane using non-conductive thread.

3. Free Space and On-body Antenna Measurements

3.1. Impedance Matching

The impedance mismatch performance for the textile HMMPA antenna was measured in free space and on the SAM phantom. As shown in Fig. 6 the $S_{11} = -21.3$ dB at 2.4 GHz in free space while there was a slight detuning when placed on-body with $S_{11} = -22$ dB at 2.44 GHz. In comparison, the copper HMMPA presented $S_{11} = -21.6$ dB at 2.45 GHz in free space while $S_{11} = -22.3$ dB at 2.46 GHz on-body showing negligible detuning. As far as the -10 dB bandwidth (BW) is concerned, the textile antenna presented a three times larger BW of 150 MHz ranging from 2.36 GHz to 2.51 GHz instead of 50 MHz for the copper antenna. In both cases, the BW is large enough to cover the entire 2.4 GHz ISM band (2.4 - 2.485 GHz).

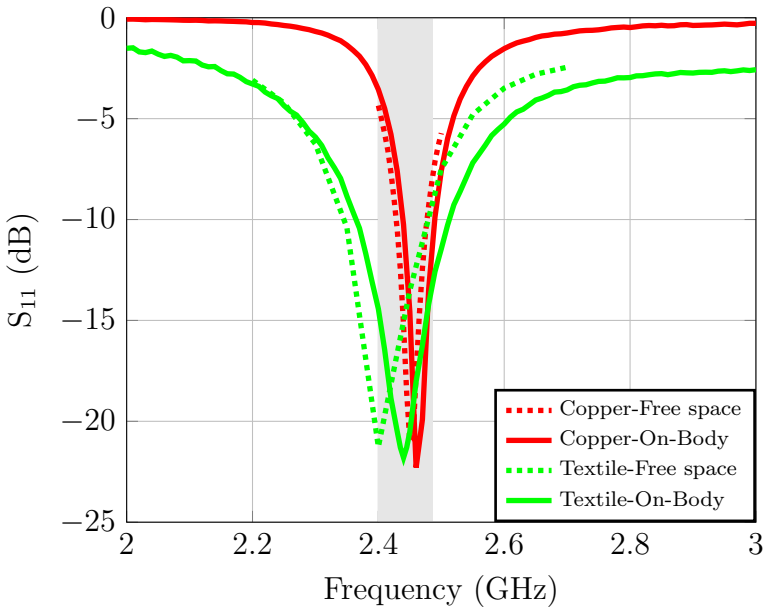

Fig. 6. *Measured reflection coefficient S_{11} of HMMPA antenna between free space (dotted line) and on-body phantom (solid line)*

3.2. Directivity, Gain and Efficiency

The far-field performance of the prototype antenna in free space was measured in an anechoic chamber using a roll-over-azimuth positioner displayed in Fig. 7a. Directivity was obtained by pattern integration while gain was acquired by using the gain transfer method.

As far as the on-body measurement is concerned, the antenna was attached on the chest of a SAM phantom with a separation distance of 10 mm (Fig. 7b). This distance was obtained

by using a Rohacell spacer and was chosen as the minimum reference distance for both antennas due the protruding SMA connector of the copper HMMPA antenna. The SAM phantom is constructed with carbon-loaded silicone rubber with dielectric properties that match body tissue over a wide frequency range (30 MHz- 6 GHz). The dielectric properties of the homogeneous body phantom material follow the MCL-T broadband tissue-equivalent recipe which is based on 2/3 muscle tissue properties, found in [27]. For the far-field on-body antenna performance, a near-field scanning technique [28] was employed. The far-field on-body coordinate system is shown in Fig. 7b.

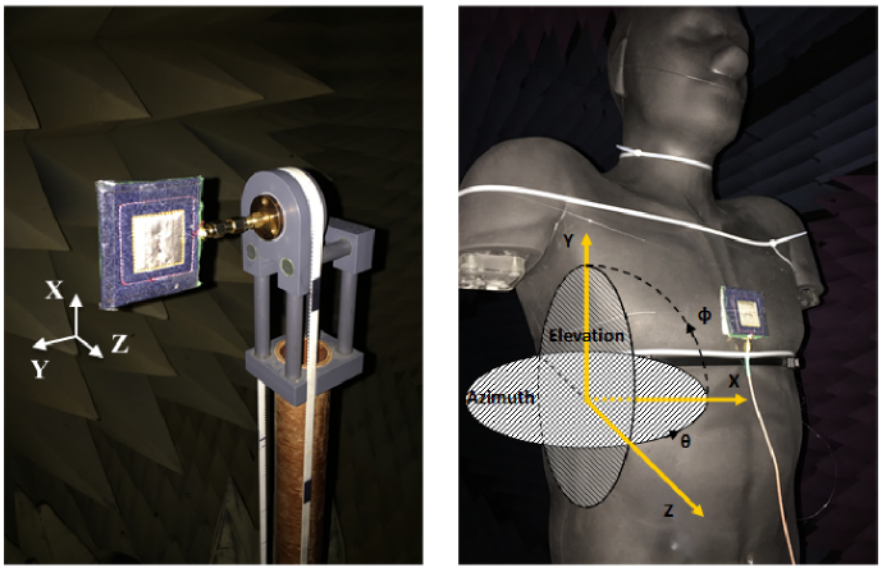

(a) (b)

Fig. 7. *Textile patch antenna in the anechoic chamber. (a) Free space, and (b) on-body measurement setup*

The HMMPA antenna directivity in free space and on-body is given in Fig. 8. It can be seen that the directivity increases when the antenna is attached on the body due to the absorption of a part of the radiated power. The textile antenna directivity is similar to the copper antenna's performance in the on-body case while this difference in the free space case is less than 1 dB.

The HMMPA antenna gain in the direction of maximum radiation ($\theta = 90^o$) is given in Fig. 9 for the textile and copper patch antennas. The gain performance of the textile patch antenna is found almost $2dB$ lower than the copper antenna in both free space and on-body cases. This is attributed to the intrinsic ohmic losses of the conductive fabric and conductive thread which form a less efficient radiator. On top of this, the textile ground plane offers less shielding than the copper sheet from the near field interaction with the phantom's body dielectric .

The measured radiation efficiency of the textile antenna in free space was more than 50% (Fig. 10b) while the copper antenna efficiency reached 88% at the resonance frequency (Fig. 10a). This difference is attributed mainly to the low conductivity of the conductive fabric and thread that were used to fabricate the textile antenna in the embroidery machine.

Comparing the measured with the simulated efficiency in Fig. 10b, a very good match-

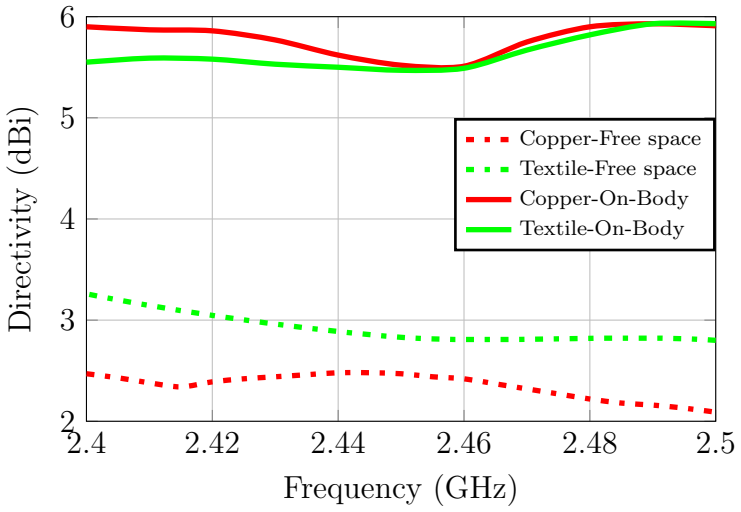

Fig. 8. *Measured directivity of the proposed textile and copper HMMPA antennas*

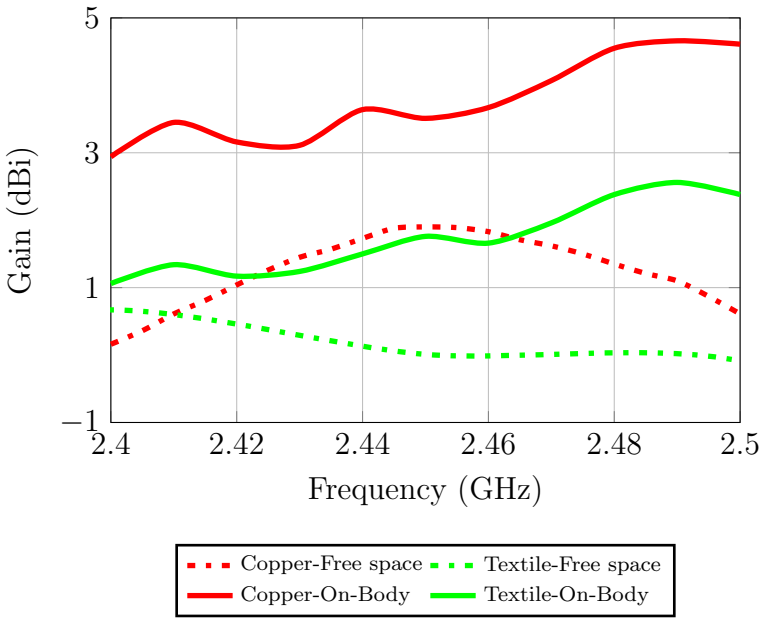

Fig. 9. *Measured maximum gain of the proposed textile and copper HMMPA antennas*

ing up to 2.44 GHz is achieved. Above this frequency, the efficiency discrepancy reaches up to 10% which is due to the accuracy of the free space measurement. By increasing the number of measurement points the difference between measurements and simulations is expected to be reduced. Moreover, an improvement on the fabrication accuracy of the textile antenna dimensions in respect to the simulated textile antenna can contribute to eliminate this difference.

More interestingly, the on-body textile antenna efficiency is reduced only by less than 15% on average compared to the free space efficiency, which is explained from the screening effect of the antenna's ground plane that minimise the severe interaction with the body. In comparison to the copper antenna performance on the body, a difference of less than 20%

on average is found, which is acceptable when talking about a fully textile antenna.

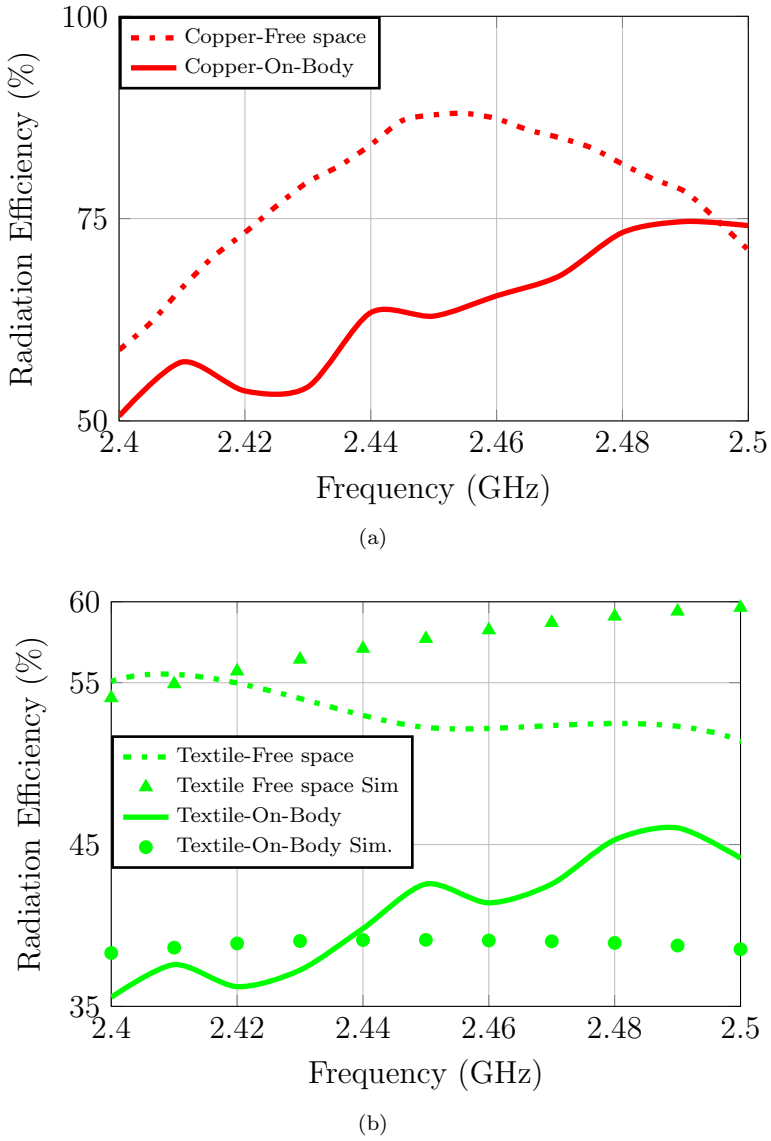

Fig. 10. *Measured and simulated radiation efficiency of the (a) copper and (b) textile HMMPA antennas*

3.3. Far-field Radiation Patterns

3.3.1. Free space radiation patterns: The far-field normalized radiation patterns for XY-, XZ- and YZ- planes are plotted in Fig. 11 for the textile (green line) and the copper (red line) antennas. The textile antenna radiation pattern is omnidirectional in the XY-plane (Fig. 11a) similar to the copper antenna pattern without being affected from the presence of the SMA connector at one of its sides ($\theta = 270^o$). In the two principal planes (Fig. 11b, 11c) the textile antenna exhibits a monopole-like radiation pattern with nulls for $\theta = 0^o$ (boresight direction) and $\theta = 180^o$ (backside direction). The null in the broadside direction of the radiation pattern indicates that the desired TM_{21} on-body mode is properly

excited while minimising the off-body radiation, as a result of the effective performance of the embroidered shorting vias. It is also seen that the cross-polar component of the textile antenna in both cases is quite low and close to the copper antenna.

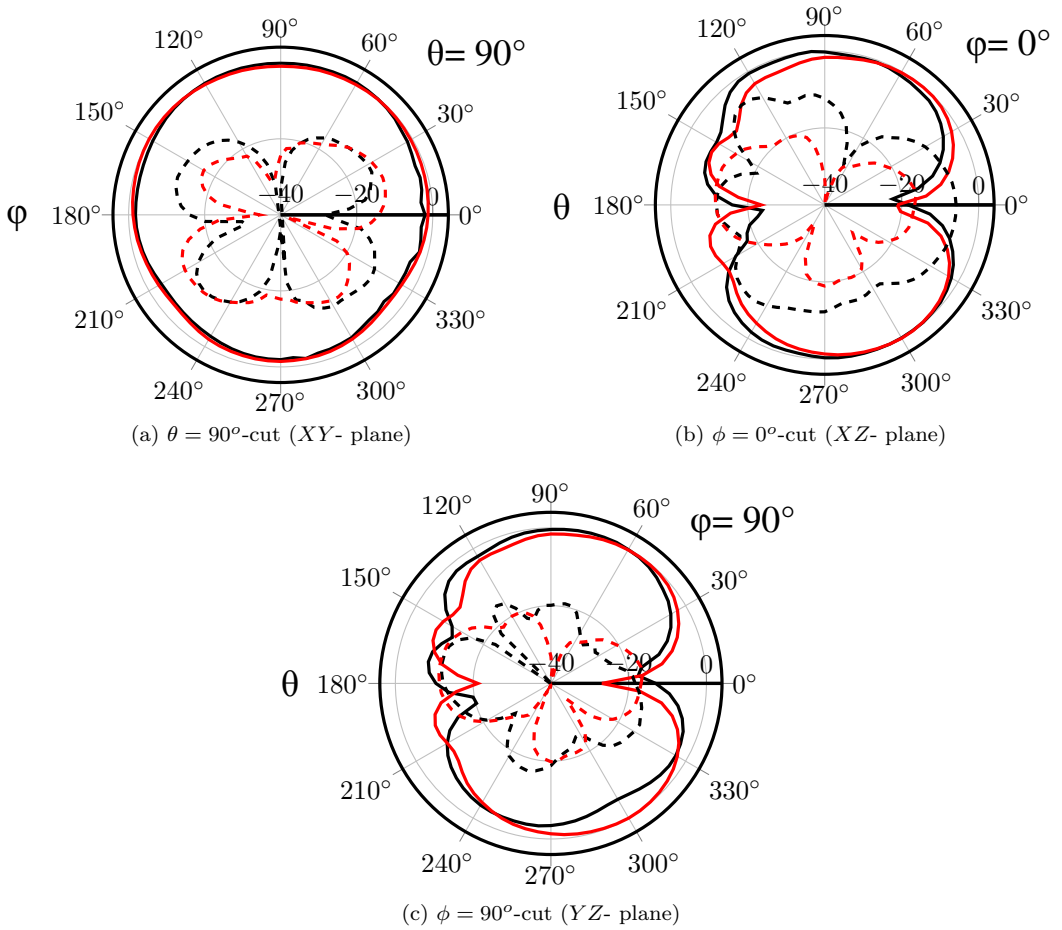

(a) $\theta = 90^o$-cut (XY- plane)

(b) $\phi = 0^o$-cut (XZ- plane)

(c) $\phi = 90^o$-cut (YZ- plane)

Fig. 11. *Measured radiation pattern for textile (black) and copper (red) HMMPA antennas in free space for co-polar. (solid) and cross-polar. (dotted) components*

3.3.2. On-Body radiation patterns: The azimuthal and elevation planes are plotted in Fig. 12. These two patterns show the normalized far-field radiation around and along the body. The radiation pattern shape of the textile antenna (black line) is almost identical to the copper one (red line) for both planes with the exception of the cross polarised component which appears slightly increased in the broadside direction. This is assigned to the bigger dielectric loading that the textile antenna experiences than the copper antenna, since the side-fed design enables to be conformal with the body.

In respect to the free space case (Fig. 11b, 11c), it is found that a part of the radiated field in the range between 90^o to 270^o is suppressed, due to the shadowing and scattering from the human body. This effect is more pronounced in the elevation plane ($\phi = 90^o$-cut) (Fig. 12b) where the shadowing effect is larger.

The proposed textile HMMPA antenna, compared with a circular patch antenna which employs electromagnetic band-gap structures to generate the on-body propagation [24],

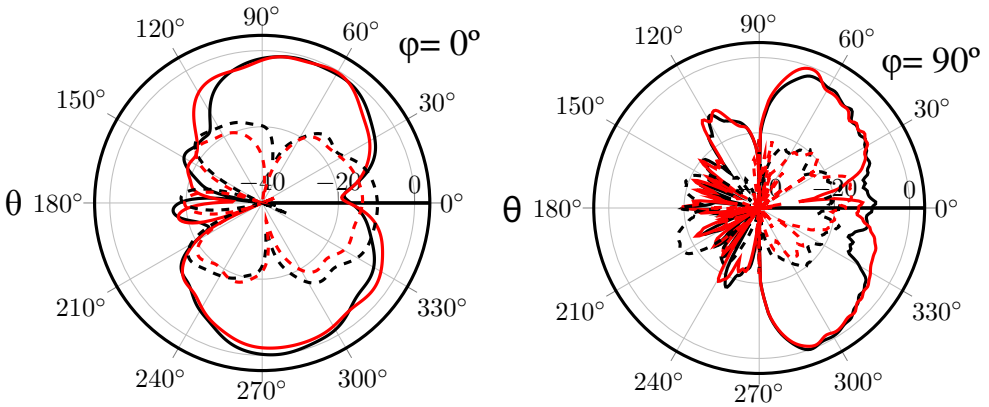

(a) $\phi = 0^o$-cut (XZ- plane) (b) $\phi = 90^o$-cut (YZ- plane)

Fig. 12. *Measured radiation pattern for textile (black) and copper (red) HMMPA antennas on torso phantom for co-polar. (solid) and cross-polar. (dotted) components*

presents an increased complexity which lies in the utilisation and implementation of the embroidered vias and the multilayer design. However, this increased complexity acts in favour of achieving a smaller size (50mm x 50 mm instead of 136mm x 136mm) and a side-fed design which gives more practicality. In addition, the proposed HMMPA achieves a better on-body coupling performance since the direction of maximum gain is located closer to the body surface ($\theta = 74^o$ for the HMMPA while $\theta = 48^o$ for the EBG antenna).

4. Conclusions

This paper proposes a flexible textile higher-mode patch antenna (HMMPA) with embroidered vias that can operate with good efficiency on the human body. It can be easily integrated in smart clothing and work together with on-body communication devices. A perpendicular to the body polarisation is obtained with a planar low-profile design. A near-field measurement has been employed to derive the efficiency and radiation patterns of the textile antenna on the human body. The radiation pattern shape of the textile antenna is found to be similar to the copper antenna, i.e. a monopole-like radiation pattern, meaning that the embroidered vias produce the desired higher order TM_{21} mode. A free space radiation efficiency of 55% is achieved while in the on-body case 46% radiation efficiency is measured for operation in the 2.4 GHz ISM band. This efficiency reduction of the HMMPA antenna in the on-body case is expected since its maximum radiation is directed along the body surface leading to a stronger interaction with the human body instead of a normal patch antenna.

5. References

[1] Salonen, P., Rahmat, Y., Hurme, H., *et al.*: 'Dual-band wearable textile antenna'. Proc. of the AP-S International Symposium of the IEEE Antennas and Propagation Society, 2004, pp. 463–466

[2] Soh, P. J., Vandenbosch, G. A. E., Ooi, S. L., *et al.*: 'Design of a broadband all-textile slotted PIFA', IEEE Transactions on Antennas and Propagation, 2012, **60**, (1), pp. 379–384

[3] Hertleer, C., Rogier, H., Vallozzi, L., *et al.*: 'A textile antenna for off-body communication integrated into protective clothing for firefighters', IEEE Transactions on Antennas and Propagation, 2009, **57**, (4), pp. 919–925

[4] Zang, L., Wang, Z., Volakis, J. L.:, 'Textile Antennas and Sensors for Body-Worn Applications', IEEE Antennas and Wireless Propagation Letters, 2012, **11**, (1), pp. 1690-1693

[5] Kaufmann, T., Fumeaux, C.: 'Wearable Textile Half-Mode Substrate-Integrated Cavity Antenna Using Embroidered Vias', IEEE Antennas and Wireless Propagation Letters, 2013, **12**, (1), pp. 805-808

[6] Seager, R., Zhang, S., Chauraya, A., *et al.*: 'Effect of the fabrication parameters on the performance of embroidered antennas', IET Microwaves, Antennas & Propagation, November 2013, **7**, (14), pp. 1174–1181

[7] Giddens, H., Paul, D. L., Hilton, G. S., *et al.*: 'Influence of body proximity on the efficiency of a wearable textile patch antenna'. Proc. of the 6th European Conference on Antennas and Propagation (EuCAP), 2012, Prague, Czech Republic, March 2012, pp. 1353–1357

[8] Nguyen, T. M., Chung, J. Y., Lee, B.: 'Radiation Characteristics of Woven Patch Antennas', IEEE Transactions on Antennas and Propagation, 2015, **63**, (6), pp. 663–666

[9] Paul, D. L., Giddens, H., Paterson, M. G., *et al.*: 'Impact of Body and Clothing on a Wearable Textile Dual Band Antenna at Digital Television and Wireless Communications Bands', IEEE Transactions on Antennas and Propagation, 2013, **61**, (4), pp. 2188–2194

[10] Hall, P.S., Hao, Y.: 'Antennas and Propagation For Body-Centric Wireless Communications' (Artech House, 2nd edn. 2012)

[11] Delaveaud, C., Leveque, P., Jecko, B.:, 'New kind of microstrip antenna: the monopolar wire-patch antenna', Electronics Letters, January 1994, **30**, (1), pp. 1-2

[12] Conway, G.A. and Scanlon, W.G.: 'Antennas for Over-Body-Surface Communication at 2.45 GHz', IEEE Transactions on Antennas and Propagation, April 2009, **57**, (4), pp. 844–855

[13] Tak, J., Kwon, K., Kim, S., *et al.*: 'Dual-Band On-Body Repeater Antenna for In-on-On WBAN Applications', International Journal of Antennas and Propagation, 2013, **2013**, (1), pp. 1-12

[14] Al-Zoubi, A., Fan, Y., Kishk, A.: 'A Broadband Center-Fed Circular Patch-Ring Antenna With a Monopole Like Radiation Pattern', IEEE Transactions on Antennas and Propagation, March 2009, **57**, (3), pp. 789-792

[15] Yang, F., Rahmat-Samii, Y., Kishk, A.: 'Low-profile patch-fed surface wave antenna with a monopole-like radiation pattern', IET Microwaves, Antennas & Propagation, February 2007, **1**, (1), pp. 261-266

[16] Liu, J., Xue, Q., Wong, H., *et al.*: 'Design and Analysis of a Low-Profile and Broadband Microstrip Monopolar Patch Antenna', IEEE Transactions on Antennas and Propagation, January 2013, **61**, (1), pp. 11-18

[17] Wong, K., Lin, C.: 'Characteristics Of a 2.4-GHz Compact Shorted Patch Antenna In Close Proximity To a Lossy Medium', Microwave and Optical Technology Letters, 2005, **45**, (6), pp. 480–483

[18] Liu, Z. G., Guo, Y. X.: 'Dual band low profile antenna for body centric communications', IEEE Transactions on Antennas and Propagation, 2013, **61**, (4), pp. 2282–2285

[19] Chen, S., Kaufmann, T., Fumeaux, T.: 'Shorting Strategies for a Wearable L-Slot Planar Inverted-F Antenna'. Proc. in the International Workshop on Antenna Technology (iWAT), April 2014, pp. 18–21

[20] Tak, J., Lee, S., Choi, J.: 'All-textile higher order mode circular patch antenna for on-body to on-body communications', IET Microwaves, Antennas & Propagation, April 2015, **9**, (6), pp. 576–584

[21] Paraskevopoulos, A., Alexandridis, A., Zervos, T., *et al.*: 'Modelling of dynamic on-body channels using different types of wearable antennas'. Proc. of the 8th European Conference on Antennas and Propagation (EuCAP), 2014, Hague, Netherlands, April 2014, pp. 852–856

[22] Paraskevopoulos, A., Alexandridis, A., Lazarakis, F, *et al.*: 'Investigation of wearable antennas performance in static LOS and NLOS on-body channels'. Proc. of Loughborough Antennas and Propagation Conference (LAPC), 2014, Loughborough, UK, Nov 2014, pp. 355–358

[23] Rahim, H., Malek, F., Adam, I., *et al*: 'Design and simulation of a wearable textile monopole antenna for body centric wireless communications'. Proc. PIERS, Moscow, Russia, August 2012, pp. 1381–1384

[24] Khouri, R., Ratajczak, P., Brachat, P., *et al*: 'A thin surface-wave antenna using a via-less EBG structure for 2.45 GHz ON-Body communication systems'. Proc. of the 4th European Conference on Antennas and Propagation (EuCAP), 2010, Barcelona, Spain, April 2010, pp. 3–6

[25] 'Nora Dell Conductive Metallized Nylon Fabric', http://www.shieldextrading.net/pdfs/NoraDell%20CR.pdf

[26] 'Liberator^{TM} conductive fiber', http://www.metalcladfibers.com/liberator-fiber

[27] 'MCL-T whole-body solid SAM phantom', http://www.mcluk.org/solid_bodies.php

[28] Yaghjian, A.D., 'Near-field antenna measurements on a cylindrical surface: A source scattering-Matrix formulation' (Dept. of Commerce, National Bureau of Standards, Institute for Basic Standards, Electromagnetics Division, Boulder, Colorado, 1977), pp. 1-38